

Metallization and magnetic order in EuB_6

S. Süllo^{1,*}, I. Prasad,^{1,†} M. C. Aronson,¹ S. Bogdanovich,^{1,‡} J. L. Sarrao,^{2,§} and Z. Fisk²

¹*Department of Physics, University of Michigan, Ann Arbor, Michigan 48109-1120*

²*National High Magnetic Field Laboratory, 1800 East Paul Dirac Drive, Florida State University, Tallahassee, Florida 32310*

(Received 9 February 2000)

We present the results of field- and temperature-dependent resistivity ρ and magnetization M measurements which show that colossal magnetoresistance in semimetallic EuB_6 is not associated with its bulk Curie temperature $T_C=12.6$ K, determined by a scaling analysis of $M(H,T)$, but with a second phase transition at $T_M=15.5$ K. We propose that metallization occurs at T_M via the overlap of magnetic polarons. The separation of the charge delocalization and bulk magnetic ordering transitions implies electronic and magnetic phase separation.

The discovery of colossal magnetoresistance (CMR) in rare-earth manganites and manganese pyrochlores has renewed interest in the properties of magnetic polarons.¹ As has often been noted, CMR was also observed in a very different class of rare-earth magnets [EuO ,² EuB_6 ,³⁻⁵ $\text{Gd}_{1-x}\text{Eu}_x\text{Se}$ (Ref. 6)] almost 30 years ago. It is generally believed that magnetic polarons are present in all of these materials, and that the sensitivity of polaronic transport to field is responsible for CMR. Although EuB_6 has historically been grouped with charge-doped rare-earth chalcogenides and oxides, in which the polaronic carriers are extrinsic, it has recently been shown that this intriguing material is a rare example of a low carrier density semimetal which also orders ferromagnetically.⁷⁻⁹ We present here a detailed study of the field- and temperature-dependent resistivity ρ and magnetization M of EuB_6 which suggests the presence of magnetic polarons in this system, and demonstrates that bulk magnetic order and metallization occur at different temperatures. This is a phenomenon unique to EuB_6 , and we will argue that it implies electronic and magnetic phase separation.

EuB_6 crystallizes in the simple cubic CaB_6 structure. The electronic structure is derived primarily from the hybridization of the boron p bands, filled by electrons donated by the Eu ions, which are found to be divalent by both photoemission¹⁰ and Mössbauer¹¹ measurements. Electronic structure calculations⁷ indicate that small dilations of the boron octohedra cause overlap of the conduction and valence bands at the X points, rendering EuB_6 semimetallic. Shubnikov-de Haas and de Haas-van Alphen measurements^{8,9} as well as angle-resolved photoemission (ARPES) measurements¹⁰ confirm that EuB_6 is a semimetal. Quantum oscillation studies found that the sample studied here has an intrinsic carrier density of $1.2 \times 10^{20} \text{ cm}^{-3}$.⁹

Neutron-diffraction measurements on EuB_6 (Ref. 12) find that the spontaneous moment first appears near ~ 16 K, increases slowly as the temperature is lowered, and then displays quasi-mean-field behavior below $\sim 12-13$ K. The saturation moment of $6.9 \pm 0.2 \mu_B$, measured at 1.5 K, is somewhat reduced from the nominal Eu^{2+} value of $7.94 \mu_B$, but is in good agreement with the $7.02 \mu_B$ predicted by band-structure calculations.⁷ Signatures of a second phase transition at 15.5 K have been found in the resistivity, the low-field magnetization, and the zero-field specific heat.^{13,14}

Currently, there is no explanation for the origin of this second transition, or its relationship to the lower temperature transition, which we will argue is a bulk ferromagnetic transition. However, the pressure dependences of both transitions indicate that the conduction electrons mediate the magnetic order of the Eu moments.¹⁵ We present here the results of resistivity and magnetization measurements which show that the CMR in EuB_6 is associated with this second, higher temperature transition, which we will call T_M . Our primary experimental conclusion is that the ferromagnetic transition at $T_C \sim 12.6$ K is preceded by a charge delocalization transition at T_M , which we will argue results from the overlap of magnetic polarons.

Large single crystals of EuB_6 were prepared from an aluminum flux, using both natural abundance Eu and B, as well as ¹⁵³Eu (94–98% enrichment) and ¹¹B. Magnetization measurements were carried out in a Quantum Design superconducting quantum interference device magnetometer. The crystals are needle shaped, and the electrical resistance was determined with the current flowing parallel to the long axis, which is a principal crystallographic direction. By comparing positive and negative field sweeps, we determined that no measurable transverse resistance was included in our measurements at any temperature.

Sample dependence is an important issue in EuB_6 , since it is a system with a very small number of intrinsic carriers. In the course of our study, we have investigated a number of samples of dramatically different qualities. Most of the results reported in this paper are from measurements carried out on the same natural abundance, single crystal used previously for quantum oscillation measurements⁹ and high resolution x-ray-diffraction¹⁴ measurements. The residual resistivity of this sample is one of the lowest reported in the literature, and the specific heat and resistive anomalies at both transitions are extremely sharp, compared to previously published reports. Further, quantum oscillation measurements on this crystal find an extremely low extrinsic carrier concentration of one hole per 185 unit cells.

We compare the electrical resistivity of this sample to that of another single crystal of EuB_6 in Fig. 1(a). The second crystal has a much higher residual resistivity, and a single, broad resistive transition. Examination of the temperature derivative of the resistivity in Fig. 1(b) reveals that the lower

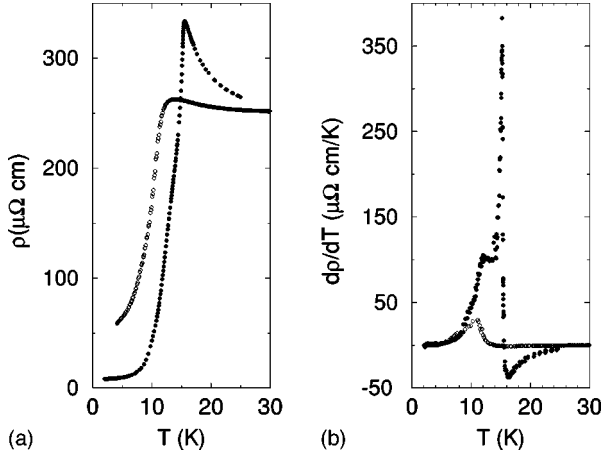


FIG. 1. A comparison of the temperature dependences of the electrical resistivity (a) and the temperature derivative of the resistivity (b) for two single crystals of EuB_6 . Most of the results reported here were obtained on the sample represented by the filled circles.

transition occurs at approximately the same temperature in the two samples, although the resistive transition is less temperature dependent in the second sample. The major difference between the two samples is that the upper transition is absent in the lower quality crystal. These results are echoed in the specific-heat measurements, shown for the two samples in Fig. 2. The dominant feature in the specific heat is the broad peak suggesting a magnetic transition at $T_C = 12.6$ K with substantial magnetic disorder. As we have previously noted,¹⁴ the Eu^{2+} moment crystal-field degeneracy is lifted by the internal field of the ferromagnet, leading to a Schottky-like anomaly at low temperatures. The apparent shift of the 12.6 K specific-heat peak to higher temperatures in the higher quality sample indicates that there is less magnetic entropy under the peak in this sample, not that T_C has changed. In addition, a distinct λ -like transition with a maximum at $T_M = 15.1$ K is seen near the upper transition in the higher quality crystal, but is absent in the lower quality crystal. We have subtracted the phonon contribution to the specific heat, and computed the temperature depen-

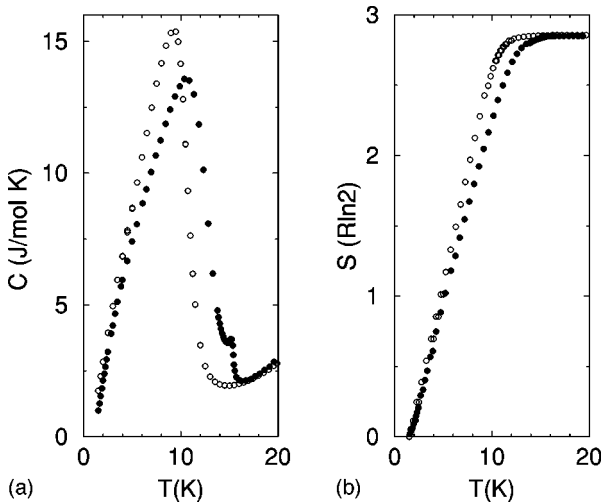


FIG. 2. A comparison of the specific heat C and the magnetic entropy S for the two samples of Fig. 1.

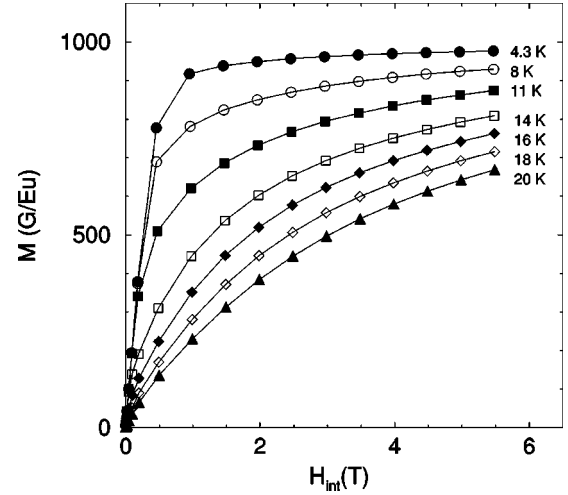


FIG. 3. The magnetization M as a function of the internal magnetic field at selected temperatures. Solid lines are guides for the eye.

dence of the entropy S in both crystals. The result is plotted in Fig. 2(b). For both samples, the entropy saturates at high temperatures at a value close to $R(3 \ln 2)$, the expected value for a mole of Eu^{2+} ions. In the lower quality crystal, the entropy saturates at T_C , while the entropy of the higher quality crystal changes more gradually with temperature, and continues to increase up to the upper transition T_M . This result indicates that the gradual decrease in entropy between T_M and T_C cannot be the result of simple disorder broadening, as the effect is more marked in the less disordered sample. We conclude from these comparisons that the higher temperature transition is much more sample dependent than the lower transition, and is only well defined in the highest quality samples.

Our first task is to determine whether ferromagnetic ordering occurs at the upper or lower transition, using an analysis of the field- and temperature-dependent magnetization. The field dependences of the magnetization for temperatures between 4.3 and 20 K are presented in Fig. 3. Here, the field is oriented along the (100) crystalline axis of the sample, and has been corrected for demagnetization effects, which are only significant below 2000 Oe. We have used Arrott plots to determine the Curie temperature and critical exponents of these data. The underlying assumption of the Arrott plot is that it is possible to expand the field H in odd powers of the magnetization M :¹⁶

$$H/M = a_0 + a_1 M^2 + a_2 (M^2)^2 + \dots \quad (1)$$

We have replotted the data of Fig. 3 as H/M as a function of M^2 in Fig. 4. The intercept of the isotherms with the horizontal axis is the square of the spontaneous magnetization of the ferromagnet M_S^2 , while the intercept with the vertical axis is χ_0^{-1} , the inverse of the zero-field susceptibility. Since demagnetization effects and domain reorientation generally dominate the low-field magnetization of ferromagnets, it is necessary to extrapolate these intercepts from the high-field magnetization. For this reason, we have omitted

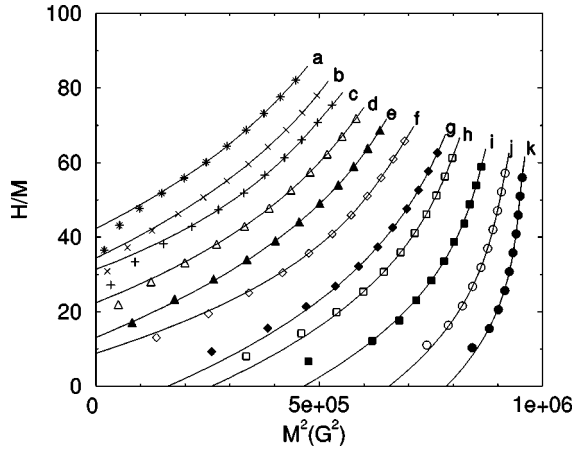


FIG. 4. Arrott plots of the magnetization isotherms. As described in the text, lines are polynomial fits to the high field, large M data. (a) 20 K, (b) 18.5 K, (c) 17.5 K, (d) 16 K, (e) 14.5 K, (f) 13 K, (g) 11 K, (h) 10 K, (i) 8 K, (j) 6.6 K, (k) 4.3 K.

data taken in fields of 2000 Oe and less. We have used third-order polynomials to generate the extrapolations which appear in Fig. 4.

The Arrott plot analysis indicates that the spontaneous moment first appears between 11 and 13 K. We can obtain an accurate value for the Curie temperature T_C by examining the temperature dependence of χ_0 , which appears in Fig. 5(a). The scaling analysis requires that χ_0 diverge as the temperature is lowered towards the ferromagnetic transition at T_C , $\chi_0(t) \propto t^{-\gamma}$, where $t = (T - T_C)/T_C$. We define the quantity $T^* = [d/dT(\ln \chi_0^{-1})]^{-1} = (T - T_C)/\gamma$, which is plotted in Fig. 5(b). A least-squares analysis gives $T_C = 12.6 \pm 0.2$ K, and $\gamma = 0.88 \pm 0.01$. As a consistency check, we see that this power law agrees well with χ_0 over more than a decade in reduced temperature, as shown in Fig. 5(a).

The spontaneous magnetization M_S extracted from the Arrott plot analysis is shown in Fig. 6(a). At the lowest temperatures, M_S approaches the $7.94 \mu_B$ expected for Eu^{2+} mo-

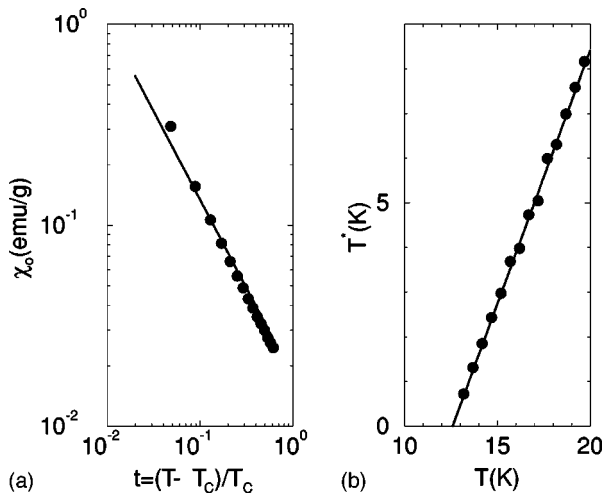


FIG. 5. (a) The extrapolated zero-field susceptibility χ_0 as a function of reduced temperature $t = (T - T_C)/T_C$. (b) The temperature intercept of T^* , defined in the text, determines the bulk ferromagnetic transition $T_C = 12.6 \pm 0.2$ K. Solid lines are least-squares fits, described in the text.

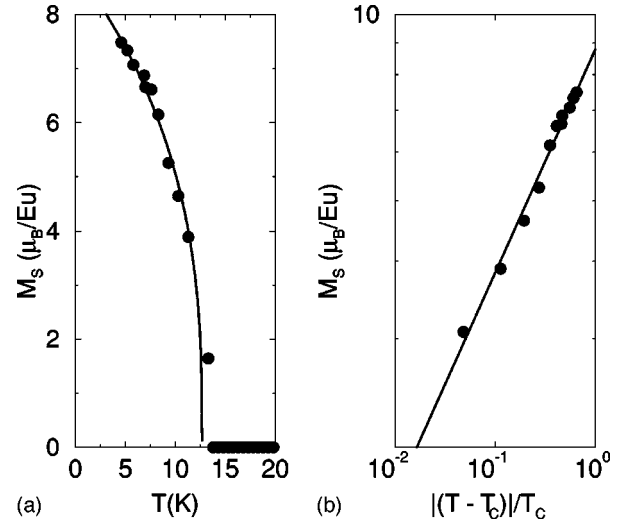


FIG. 6. (a) The temperature dependence of the spontaneous moment determined by the Arrott plot analysis. The line is a power-law fit using $T_C = 12.6$ K. (b) The spontaneous moment obeys a power law in reduced temperature (solid line) with a slope $\beta = 0.36 \pm 0.013$.

ments. In the ferromagnetic phase, $M_S \propto |t|^{-\beta}$. As demonstrated in Fig. 6(b), we find $\beta = 0.36 \pm 0.02$, using $T_C = 12.6 \pm 0.2$ K. Again, the results of this power-law fit are compared to $M_S(T)$ in Fig. 6(a).

The most stringent test of the scaling hypothesis is whether the magnetization curves can be described by the expression

$$M(H, t) = t^\beta f(H/t^{\gamma+\beta}) \quad (2)$$

for a wide range of the scaling variable $H/t^{\gamma+\beta}$. All the magnetization data with $T \geq 13$ K have been replotted as $Mt^{-\beta}$ as a function of $H/t^{\gamma+\beta}$ in Fig. 7 using the values $T_C = 12.6$, $\beta = 0.36$, and $\gamma = 0.88$, taken from the Arrott plot

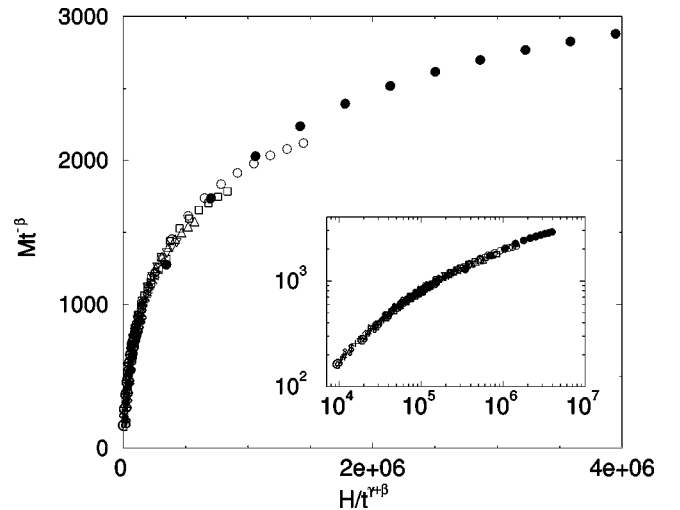


FIG. 7. Scaling of the magnetization M for fields $H \geq 0.2$ T, and $T \geq T_C = 12.6$ K. All fields have been corrected for demagnetization effects. 13 K (\bullet), 13.5 K (\circ), 14 K (\square), 14.5 K (\triangle), 15 K (∇), 15.5 K (\langle), 16 K (\triangleright), 16.5 K (\diamond), 17 K ($*$), 17.5 K ($+$), 18 K ($\$$), 18.5 K ($\%$), 19 K ($\#$), 19.5 K ($!$), and 20 K ($@$). Inset: The same quantities in a double log plot.

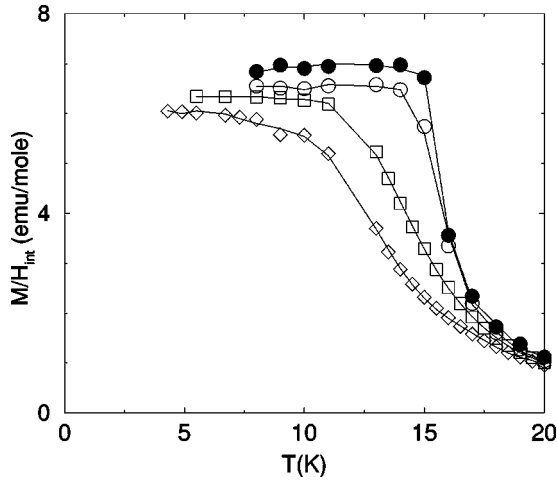


FIG. 8. M/H_{int} for fields of 75 G (●), 200 G (○), 1000 G (□), and 2000 G (◇). Solid lines are guides for the eye.

analysis. The scaling is excellent, and the inset to Fig. 7 shows that the scaling extends over almost three decades of the scaling variable $H/t^{\gamma+\beta}$.

In summary, our analysis of the magnetization of EuB_6 in fields greater than 2000 Oe reveals that bulk ferromagnetic order occurs at the lower transition, $T_C = 12.6 \pm 0.2$ K. This result is in agreement with the neutron-diffraction measurement¹² as well as with the presence of a large, but broad, specific-heat anomaly found near this temperature.¹⁴ The critical exponent $\beta = 0.36 \pm 0.02$ agrees well with theoretical estimates for the three-dimensional Heisenberg model, 0.365 ± 0.003 .¹⁷ However, the value for the exponent $\gamma = 0.88 \pm 0.01$ is in poor agreement with either the mean-field value $\gamma = 1$, or the three-dimensional Heisenberg model $\gamma = 1.336 \pm 0.004$. As we will argue below, we believe that this discrepancy may result from phase separation in EuB_6 in the paramagnetic state, although the ferromagnetic state with $T \leq T_C$ is homogeneous.

We stress that this scaling analysis is limited to fields above 2000 Oe, and has nothing to say about the low-field behavior. Magnetization measurements in very low fields indicate the onset of a small spontaneous moment at the upper transition as well, just as was found in the neutron-diffraction measurement.¹² To demonstrate this, we have plotted M/H_{int} as a function of temperature for demagnetization corrected fields H_{int} ranging from 75–2000 Oe in Fig. 8. We have previously reported the detailed field dependences of this transition.¹⁴ In the lowest fields M/H_{int} increases sharply near 15.5 K, while increased fields rapidly broaden and suppress the transition. The detailed temperature dependences of $M/H_{int}(T)$ can be quantitatively affected by uncertainties in the demagnetization corrections, as well as by the possibility of inhomogeneous field penetration in our nonellipsoidal sample. However, the rapid increase in M/H_{int} below 15.5 K in low fields is a robust result, and indicates the presence of a spontaneous moment. Since an Arrott plot analysis is impossible in this field range, we cannot determine the magnitude of the spontaneous moment associated with the higher temperature transition. However, the entropy associated with the 15.5 K specific-heat anomaly in this sample is approximately 15% of the total $R \ln 8$ measured at and below 15 K. Assuming this is entirely magnetic

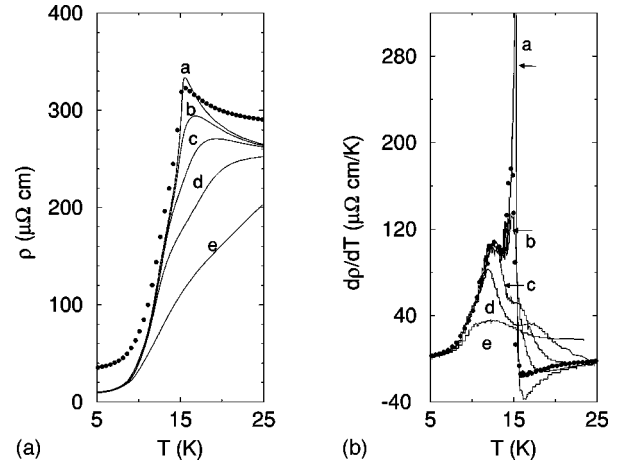


FIG. 9. (a) The temperature dependence of the resistivity ρ of EuB_6 in zero field (a) and in fields of 0.05 T (b), 0.1 T (c), 0.2 T (d), 0.5 T (e). $^{153}\text{Eu}^{11}\text{B}_6$ (●) (b) The temperature derivative of the resistivity for the same fields, as well as for $^{153}\text{Eu}^{11}\text{B}_6$ (●) at zero field. The larger residual resistivity ($34 \mu\Omega \text{ cm}$) and broadened transition of the latter indicate that it is the lower quality crystal.

entropy, this suggests that approximately 15% of the Eu moments order at the higher temperature transition, and the remainder at the 12.6 K bulk transition. In addition, Fig. 8 suggests that magnetic fields suppress the spontaneous moment at T_M . It would be of interest to test these conclusions by repeating the neutron-diffraction experiment with greater emphasis on temperatures between T_M and T_C , comparing results in zero field and in fields larger than 2000 Oe.

The field and temperature dependences of the electrical resistivity show that charge transport is much more strongly affected by the 15.5 K transition than by the 12.6 K bulk ferromagnetic transition. The temperature dependences of the electrical resistivity in fixed external fields ranging from 0.05–0.5 T are presented in Fig. 9(a). In zero field, the resistance drops more than a factor of 30 from its value of $\sim 330 \mu\Omega \text{ cm}$ just above the Curie temperature to its residual value of $8.7 \mu\Omega \text{ cm}$ at 1.2 K. The magnitude of this resistance drop is consistent with the loss of spin disorder scattering, and as expected, Fig. 9(a) shows that magnetic fields rapidly suppress the resistance drop. In a normal metallic ferromagnet, the temperature derivative of the critical scattering resistivity $\partial\rho/\partial T$ is a maximum at the Curie temperature.¹⁸ The presence of two phase transitions is dramatically revealed in Fig. 9(b), where we have plotted $\partial\rho/\partial T$ at different fields. The field dependences of the resistivity near the two transitions are very different. Magnetic fields modestly suppress the critical scattering found near the 12.6 K Curie temperature and broaden the transition. In contrast to this typical ferromagnetic behavior, the resistance near the upper transition is more rapidly suppressed, and the transition is dramatically broadened and shifted to larger temperatures. Figure 9(b) demonstrates that the maximum magnetoresistance occurs not at the lower temperature bulk ferromagnetic transition, but rather at the 15.5 K transition. The transition, which we define by the maximum in $\partial\rho/\partial T$ is 15.5 K in zero field and increases to 17.2 K in 0.2 T.

We have also measured the zero-field resistance of a single crystal of EuB_6 prepared with ^{153}Eu and ^{11}B , and the results are plotted in Figs. 9(a) and 9(b). The residual resis-

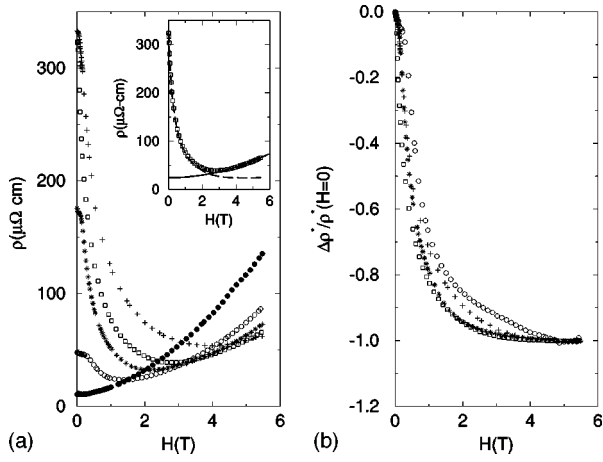


FIG. 10. (a) The magnetoresistivity $\rho(H)$ at 4.9 K (\bullet), 10 K (\circ), 13 K ($*$), 15.5 K (\square), and 20 K ($+$). The inset illustrates the procedure to extract the magnetic contribution ρ^* from the total magnetoresistivity for the data at 15.5 K: (\square) total resistivity $\rho(H)$; (solid line) metallic magnetoresistivity $\propto H^2$; (dashed line) magnetic magnetoresistivity ρ^* . The normalized $\Delta\rho^*(H)/\rho^*(0)$ at the same temperatures is shown in (b).

tivity of this sample is $34 \mu\Omega \text{ cm}$, suggesting a larger amount of disorder than in the natural abundance sample studied here. Figure 9(b) shows that neither of the resistive transitions displays a measurable isotope effect.

Magnetic fields have the largest effect on the resistivity near the higher temperature transition. We have plotted the resistance as a function of demagnetization corrected field H_{int} at several fixed temperatures in Fig. 10(a). At the lowest temperatures, the magnetoresistance is positive and quadratic in field, representing the metallic magnetoresistance ubiquitous in conducting hexaborides.^{9,19,20} As the temperature is raised, a negative contribution to the magnetoresistance appears at low fields, whose magnitude increases to a maximum near the 15.5 K transition. As demonstrated in the inset of Fig. 10(a), above 8 K it is possible to isolate the negative part of the magnetoresistance, ρ^* , by fitting and subtracting the high field, magnetoresistance, $\rho_{met} \propto H^2$, from the measured $\rho(H, T)$. The normalized magnetoresistance $\Delta\rho^*/\rho^*(H=0)$ is plotted in Fig. 10(b) at different temperatures. At every temperature, $\Delta\rho^*/\rho^*(H=0)$ approaches -1 in high fields, indicating that the zero field magnetic magnetoresistance is completely suppressed. As Fig. 10(b) indicates, this is accomplished in the smallest fields when the temperature is near T_M . The low-field magnetoresistance near T_M is similar to those found in other CMR compounds,^{1,2,6} including rare-earth manganites.

A comparison of the field- and temperature-dependent resistivity and magnetization is consistent with the resistivity originating with spin disorder scattering from the magnetic background, which we have shown is critical at $T_C = 12.6$ K. Figure 11 details the relationship between the absolute value of $\Delta\rho^*/\rho^*$ and M at different temperatures, with magnetic field as the implicit variable. For temperatures above 15 K, data at fields from 0.2–5 T fall onto a single curve $\Delta\rho^*/\rho^*(M/M_{0,0})$, where $M_{0,0}$ is the zero-temperature spontaneous moment, taken to be $6.9\mu_B$ per Eu. For $T \leq 15$ K, $\Delta\rho^*/\rho^*$ is initially almost independent of magnetization, suggestive of ferromagnetic intergranular scattering,

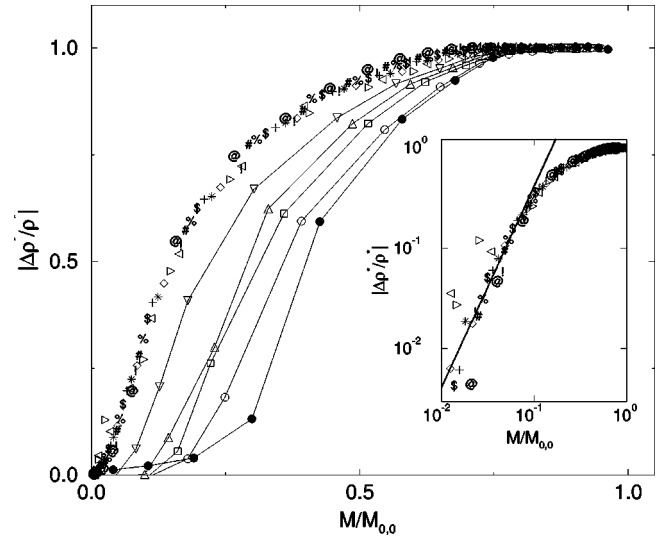


FIG. 11. The absolute value of the magnetic magnetoresistivity $\Delta\rho^*/\rho^*(H=0)$ vs the normalized magnetization $M/M_{0,0}$. Symbols have the same meaning as in Fig. 7. The inset displays the data between 15 and 20 K. The solid line represents $\Delta\rho^*/\rho^*(H=0) = C(M/M_{0,0})^2$, with $C = 75 \pm 20$ for $M/M_{0,0} < 0.07$.

but eventually rejoins the universal curve at a value of $M/M_{0,0}$ which increases with decreasing temperature. The inset of Fig. 11 compares the absolute value of $\Delta\rho^*/\rho^*(0)$ with the theoretical expression for spin disorder scattering in low fields: $\Delta\rho^*/\rho^*(0) = C(M/M_{0,0})^2$. The agreement is reasonable for $M/M_{0,0} \leq 0.07$ and gives $C = 75 \pm 20$. The same qualitative relationship is found in the rare-earth manganites.²¹ While C is expected to increase with decreasing carrier concentration,^{22,23} the value in EuB_6 is at least an order of magnitude larger than these theories predict, given the known carrier concentration.

It follows from our analysis of the scaling properties of $M(H, T)$ and from the relationship between $\Delta\rho^*/\rho^*$ and $M/M_{0,0}$ in Fig. 11 that $\Delta\rho^*/\rho^*$ can also be scaled with H and reduced temperature $t = (T - T_C)/T_C$, with $T_C = 12.6$ K. As Fig. 11 suggests, it is not possible to achieve a satisfactory data collapse if we choose the critical temperature to be 15.5 K. This implies a very powerful and perhaps surprising result about the 15.5 K metallization transition. Specifically, at temperatures greater than 15.5 K, carriers are scattered by magnetic fluctuations which are critical at 12.6 K, not 15.5 K. In essence, the incipient divergence in the resistance associated with the bulk ferromagnetic transition at 12.6 K is cut off by a sudden metallization transition at 15.5 K, whose onset temperature is itself extremely sensitive to magnetic fields.

The picture which emerges from the resistivity and magnetization data is quite unique. EuB_6 undergoes a bulk ferromagnetic transition at 12.6 K, which impacts the resistivity only modestly. In contrast, the higher temperature transition at 15.5 K is marked by the appearance of a weak spontaneous moment. Specific-heat measurements indicate that the great majority of the Eu moments order at 12.6 K, and that approximately 15% of the moments are affected by the upper transition. The most dramatic signature of the higher temperature transition is in the electrical resistivity, which is exquisitely sensitive to variations in both temperature and

field. In the most essential terms, EuB_6 makes a transition at 15.5 K from a localized and poorly conducting paramagnetic state to a delocalized and metallic state with a small spontaneous moment. The primary effect of magnetic field is to suppress this higher temperature transition, approaching a bulk phase transition near 12.6 K in high fields.

So far, we have not offered an explanation for the microscopic origin of this higher temperature transition. We argue here that this transition is from a high-temperature state of isolated and localized carriers, which we will suggest are magnetic polarons, to a low-temperature conducting state, resulting from the overlap of these polarons. We are not the first to suggest that magnetic polarons are present in EuB_6 . Twenty years ago Kasuya proposed⁵ that magnetic polarons are a ubiquitous feature of low carrier density systems with localized magnetic moments. While the argument at that time for magnetic polarons in EuB_6 was essentially an analogy to related systems such as EuO and $\text{Eu}_{1-x}\text{Gd}_x\text{Se}$, sufficient experimental and theoretical information has accrued in the ensuing years to make this argument explicit for EuB_6 . Magnetic polarons are stabilized when it is energetically favorable for the carriers to spin polarize the local moments over a finite distance, with the increased energy of the spin system compensated by the reduced kinetic energy of the carrier, which is subsequently localized in the polaron. In contrast to the Jahn-Teller-assisted double-exchange process found in the manganites,²⁴ a local lattice deformation is not required for this purely magnetic polaron.

There are a number of observations in EuB_6 which are consistent with the presence of magnetic polarons above T_M . While the resistance near room temperature in EuB_6 is metallic, and originates primarily from spin disorder scattering,¹⁵ there is a broad minimum near 100 K and the resistance begins to increase as the temperature is lowered towards T_M . Except very near T_M , where Fig. 11 shows that the resistance is primarily spin disorder scattering, we suggest that the increase in resistance with decreasing temperature is the result of charge localization by means of magnetic polaron formation. In agreement with this suggestion, Fig. 9 shows that magnetic fields suppress the resistance on this temperature interval, increase T_M , and reduce the energy barrier evidenced in the temperature-dependent scattering, all as expected for magnetic polarons. More direct evidence for isolated polarons above T_M comes from Raman scattering,²⁵ which finds two field sensitive modes, whose symmetry properties are those expected for magnetic polarons. Since these new modes are observed below 30 K, we adopt this value as an estimate for the polaron formation temperature.

We suggest that the narrowness of the semimetallic bands is the primary energetic factor which makes magnetic polarons possible in EuB_6 . Figure 9(b) shows that both T_C and T_M , taken from the zero field dp/dT for $^{153}\text{Eu}^{11}\text{B}_6$ and natural abundance EuB_6 single crystals, are identical, confirming a minimal role for lattice strain. Instead, polaron stability is controlled by two energy scales:²⁶ the local moment-conduction electron exchange (IS), and the conduction electron bandwidth E_o . We estimate the former to be 0.24 eV by equating the measured 330 $\mu\Omega\text{-cm}$ found above T_M , less an estimated 165 $\mu\Omega\text{-cm}$ of field-independent lattice resistivity, to the spin disorder scattering.²⁷ ARPES measurements¹⁰ and band-structure calculations⁷ give E_o

$=0.25$ eV. These values yield an estimate of the polaron onset temperature of 230 K. It is only necessary to decrease IS by a factor of 2, consistent with experimental uncertainties, to obtain the 30 K onset temperature observed in the Raman measurement.²⁵ The magnetic polarons have a calculated radius at formation of \sim two lattice constants, where they occupy \sim 10% of the sample volume.

Enhancing the local moment magnetization by lowering the temperature or increasing the magnetic field increases the size of magnetic polarons, and, we suggest, can lead to their metallization via overlap. Polaron overlap is marked in EuB_6 by the drop in resistivity at T_M , and by the accompanying rapid increase in carrier number or decrease in carrier mass implied by zero-field optical reflectivity measurements.¹³ While a small spontaneous moment is found at T_M , the bulk ferromagnetic transition occurs at 12.6 K. The separation of the charge delocalization and bulk magnetic ordering temperatures is a phenomenon unique to EuB_6 , and is not observed in rare-earth manganites or the doped rare-earth chalcogenides.²⁸ We propose that at 15.5 K the EuB_6 phase separates into a conducting and ferromagnetically ordered phase coexisting with a paramagnetic and poorly conducting majority phase. Our proposal is that the conducting phase results from the overlap of magnetic polarons, and forms a percolating, low resistance path across the otherwise insulating sample at 15.5 K. The magnetic signature at T_M is commensurate with the small number of moments involved in this conducting and ferromagnetic phase, estimated from the specific-heat anomaly as approximately 15% of all Eu moments. This is less than the cubic lattice percolation limit, and we speculate that the entropy gain associated with the delocalization of the carriers makes up the difference. As the temperature is lowered from 15.5 to 12.6 K, the volume fraction of the conducting, ferromagnetic phase increases at the expense of the paramagnetic phase, until the sample becomes homogeneous, conducting, and a bulk ferromagnet at 12.6 K. The gradual development of the homogeneous phase is mirrored in the unusually slow freezeout of entropy found between T_M and T_C . Finally, we hypothesize that the absence of a well-defined polaron metallization transition in highly disordered samples (Figs. 1 and 2) may result from the inability of the sample to generate both a percolating conducting path and a substantial correlation length for ferromagnetic order at other than the bulk transition.

Magnetic field is expected to increase polaron size, and the field dependence of T_M suggests that the polaron dimensions are the same whether the overlap transition occurs in zero field at 15.5 or at 17.2 K in a field of 0.2 T. We estimate that $T_M(H)$ intersects the polaron stabilization temperature $T_{pol}(H)$ at \sim 31 K and 1.5 T. In zero field, polarons decompose into free carriers as the temperature is raised above $T_{pol} \approx 30$ K,²⁵ but in 0.5 T and for temperatures below 31 K the polarons are so large that metallization accompanies polaron formation. The quantum oscillation measurements⁹ support this view, finding an almost constant carrier concentration and effective mass at all temperatures. This is reasonable, as the high fields in which these measurements are performed far exceed the metallization field at any temperature below 31 K.

We have presented here a detailed study of the relationship between transport and magnetization in EuB_6 , which is

consistent with the presence of magnetic polarons. We show that the zero-field ferromagnetic transition occurring at 12.6 K is preceded by charge delocalization at 15.5 K. EuB_6 is unique among polaronic hosts because its intrinsic carriers themselves mediate the magnetic interactions among localized Eu moments. We propose that EuB_6 finds a unique compromise between magnetic order and charge localization, not possible in higher carrier concentration magnets. Namely, the carrier and magnetic entropies can be reduced by ordering *part* of the sample, with the energy differential of the magnetic moments accommodated by the localization of carriers. The remainder of the sample orders at a lower, bulk

temperature. It appears that this sort of electronic phase separation is ultimately untenable if the overall carrier concentration is increased by pressure or doping, or if the polaron size is enhanced by field. The system then reverts to a homogeneous magnetic state, found in relatively high carrier concentration metallic magnets with polarons, such as rare-earth manganites.

We thank P. Thalmeier, S. L. Cooper, P. Littlewood, A. J. Millis, and J. W. Allen for useful discussions. Work at the University of Michigan was supported by the U.S. Department of Energy, Office of Basic Energy Sciences, under Grants No. 94-ER-45526 and 97-ER-2753.

*Present address: Dept. of Physics, TU Braunschweig, Braunschweig, Germany.

†Present address: Harvard Univ., Cambridge, MA 02138.

‡Present address: NHMFL, Tallahassee, FL 32310.

§Present address: Los Alamos National Laboratory, Los Alamos, NM 87545.

¹For reviews, see A. P. Ramirez, *J. Phys.: Condens. Matter* **9**, 8171 (1997); M. A. Subramanian *et al.*, *Science* **273**, 81 (1996).

²J. B. Torrance *et al.*, *Phys. Rev. Lett.* **29**, 1168 (1972); M. R. Oliver *et al.*, *Phys. Rev. B* **5**, 1078 (1972).

³Z. Fisk *et al.*, *J. Appl. Phys.* **50**, 1911 (1979).

⁴C. N. Guy *et al.*, *Solid State Commun.* **33**, 1055 (1980).

⁵T. Kasuya *et al.*, *Solid State Commun.* **8**, 1543 (1970); T. Kasuya *et al.*, *J. Phys. (Paris), Colloq.* **41**, C5-161 (1980).

⁶S. von Molnar and S. Methfessel, *J. Appl. Phys.* **38**, 959 (1967).

⁷S. Massidda *et al.*, *Z. Phys. B: Condens. Matter* **102**, 83 (1997).

⁸R. G. Goodrich *et al.*, *Phys. Rev. B* **58**, 14 896 (1998).

⁹M. C. Aronson *et al.*, *Phys. Rev. B* **59**, 4720 (1999).

¹⁰J. A. Clack *et al.* (unpublished).

¹¹M. Abd-Elmeguid *et al.* (unpublished).

¹²W. Henggeler *et al.*, *Solid State Commun.* **108**, 929 (1998).

¹³L. Degiorgi *et al.*, *Phys. Rev. Lett.* **79**, 5134 (1997).

¹⁴S. Süllow *et al.*, *Phys. Rev. B* **57**, 5860 (1998).

¹⁵J. C. Cooley *et al.*, *Phys. Rev. B* **56**, 14 541 (1997).

¹⁶J. S. Kouvel and M. E. Fisher, *Phys. Rev.* **136**, A1626 (1964).

¹⁷V. Privman *et al.*, in *Phase Transitions and Critical Phenomena*, edited by C. Domb and J. L. Lebowitz (Academic, New York, 1991), p. 1.

¹⁸M. E. Fisher and J. S. Langer, *Phys. Rev. Lett.* **20**, 665 (1968).

¹⁹J. C. Cooley *et al.*, *Phys. Rev. B* **52**, 7322 (1995); (unpublished).

²⁰A. J. Arko *et al.*, *Phys. Rev. B* **13**, 5240 (1976).

²¹M. F. Hundley *et al.*, *Appl. Phys. Lett.* **67**, 860 (1995); J. Z. Sun *et al.*, *ibid.* **67**, 2726 (1995).

²²N. Furukawa, *J. Phys. Soc. Jpn.* **63**, 3214 (1994).

²³P. Majumdar and P. Littlewood, *Nature (London)* **395**, 479 (1998); *Phys. Rev. Lett.* **81**, 1314 (1998).

²⁴A. J. Millis, *Nature (London)* **392**, 147 (1998); A. J. Millis *et al.*, *Phys. Rev. Lett.* **74**, 5144 (1995); G. Zhao *et al.*, *Nature (London)* **381**, 676 (1996); N. A. Babushkina *et al.*, *ibid.* **391**, 159 (1998).

²⁵P. Nyhus *et al.*, *Phys. Rev. B* **56**, 2717 (1997).

²⁶A. Yanase, *Int. J. Magn.* **2**, 99 (1972).

²⁷P. G. de Gennes, *J. Phys. Radium* **23**, 510 (1962).

²⁸We note that metallization occurs in EuO below the ferromagnetic transition (Ref. 2) and is thought to result from a small to large polaron crossover which is destabilized by spin waves [D. Emin *et al.*, *Phys. Rev. B* **35**, 641 (1987)].